Supplementary Material for

Lagrangian Tracking of Moisture Sources for the Record-Breaking Rainfall of Storm Ianos

Patricia Coll-Hidalgo[1], Raquel Nieto[1,2], Alexandre Ramos[3], Patrick Ludwig[3], Luis Gimeno[1,2]

[1]Centro de Investigación Mariña, Universidade de Vigo, Environmental Physics Laboratory (EPhysLab), Campus As Lagoas s/n, 32004 Ourense, Spain.

[2]Galicia Supercomputing Center (CESGA), Santiago de Compostela, Spain
[3]Institute of Meteorology and Climate Research (IMKTRO), Karlsruhe Institute of Technology (KIT), Karlsruhe, Germany

Correspondence to: Patricia Coll-Hidalgo (patricia.coll@uvigo.es)

SECTION A: Cyclone phase space

Figure S1: Time series of upper-level thermal wind (VTU, top) between 300–600 hPa, low-level thermal wind (VTL, middle) between 600–900 hPa and the thickness symmetry (B) between 600–925 hPa. The dashed black line indicates the thresholds for transition: B > 10 indicate an anti-symmetric (frontal) core and B < 10 is a symmetric core. Values for VTL and VTU above zero denote a warm core and below a cold core. Radius of parameter computation: 250 km.

Figure S2: From WRF configuration with gridded nudging activated above the PBL: time series of upper-level upper thermal wind (VTU, top) between 300–600 hPa, low-level thermal wind (VTL, middle) between 600–900 hPa and the thickness symmetry (B) between 600–925 hPa. The dashed black line indicates the thresholds for transition: B > 10 indicate an anti-symmetric (frontal) core and B < 10 is a symmetric core. Values for VTL and VTU above zero denote a warm core and below a cold core.

SECTION B: Evaluation and Performance Verification of WRF Model

Figure S3: Mean Bias Error (MBE) of the WRF model configuration with grid nudging applied above the planetary boundary layer (PBL), evaluated against ERA5 reanalysis data at 1000 hPa for various atmospheric variables. Statistically significant differences, determined at the 95% confidence level using the Wilcoxon signed-rank test, are marked with dots.

Figure S4: Similar to Figure S3, but for 850 hPa.

Figure S5: Similar to Figure S3, but for 500 hPa.

Figure S6: Similar to Figure S3, but for 200 hPa.

Figure S7: Spatial verification of precipitation for the WRF model configuration with gridded nudging above the PBL. The reference dataset used is the Multi-Source Weighted-Ensemble Precipitation (MSWEP, Beck et al., 2019).

Section C: Dynamics of Moisture Uptake

Reference

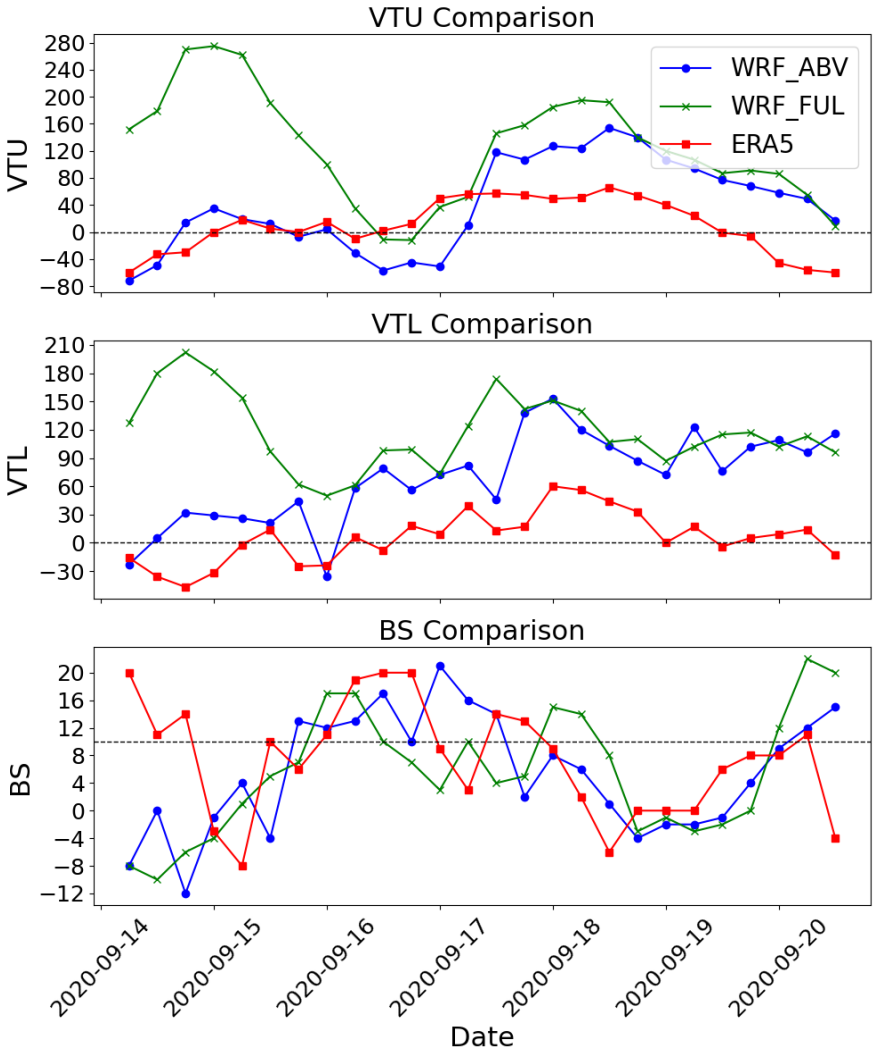

Figure S1: Time series of upper-level thermal wind ($V_T{}^U$, top) between 300–600 hPa, low-level thermal wind ($V_T{}^L$, middle) between 600–900 hPa and the thickness symmetry (B) between 600–925 hPa. The dashed black line indicates the thresholds for transition: B > 10 indicate an anti-symmetric (frontal) core and B < 10 is a symmetric core. Values for $V_T{}^L$ and $V_T{}^U$ above zero denote a warm core and below a cold core. Radius of parameter computation: 250 km.

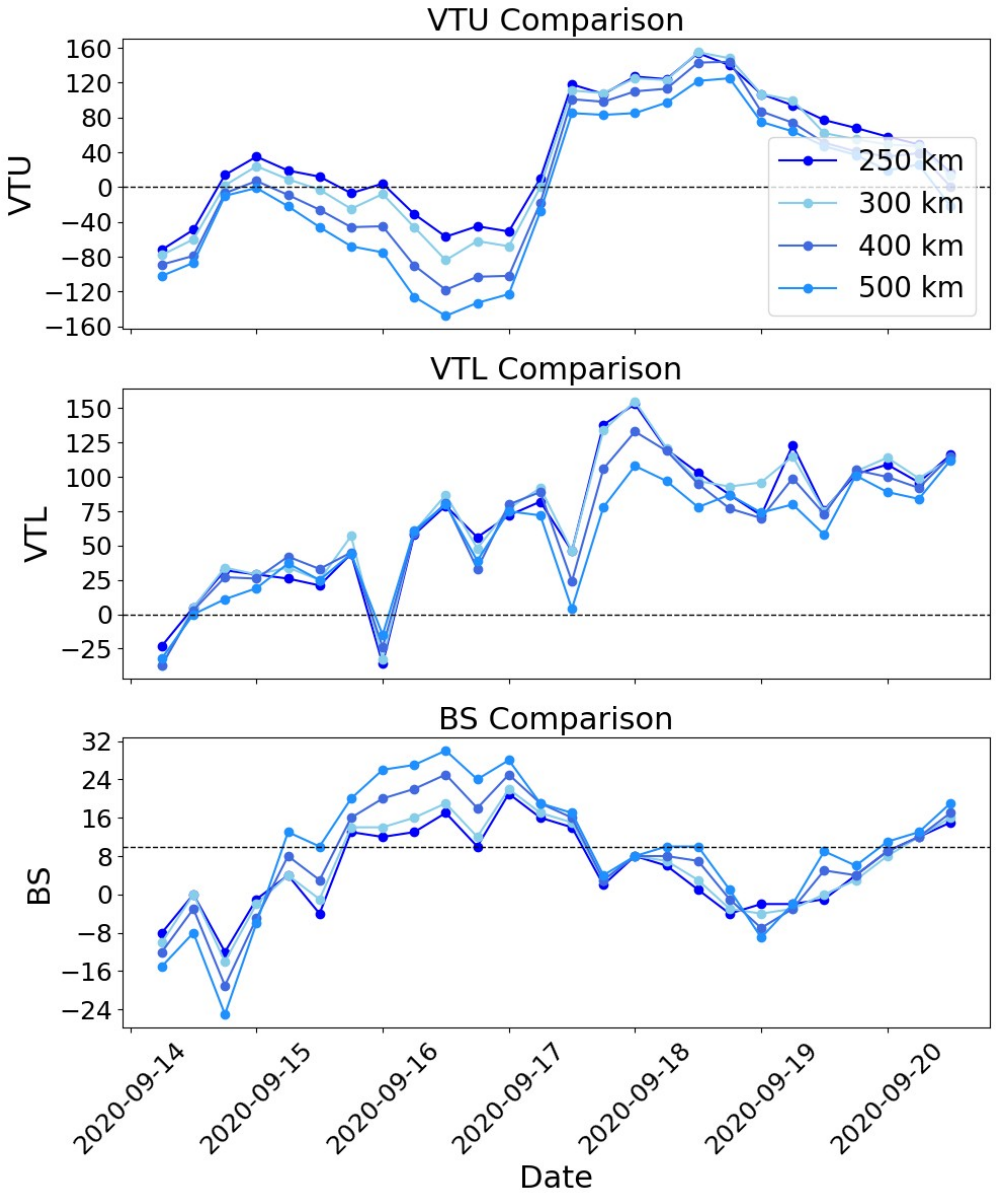

Figure S2: From WRF configuration with gridded nudging activated above the PBL: time series of upper-level upper thermal wind ($V_T{}^U$, top) between 300–600 hPa, low-level thermal wind ($V_T{}^L$, middle) between 600–900 hPa and the thickness symmetry (B) between 600–925 hPa. The dashed black line indicates the thresholds for transition: B > 10 indicate an anti-symmetric (frontal) core and B < 10 is a symmetric core. Values for $V_T{}^L$ and $V_T{}^U$ above zero denote a warm core and below a cold core.

SECTION B: Evaluation and Performance Verification of WRF Model

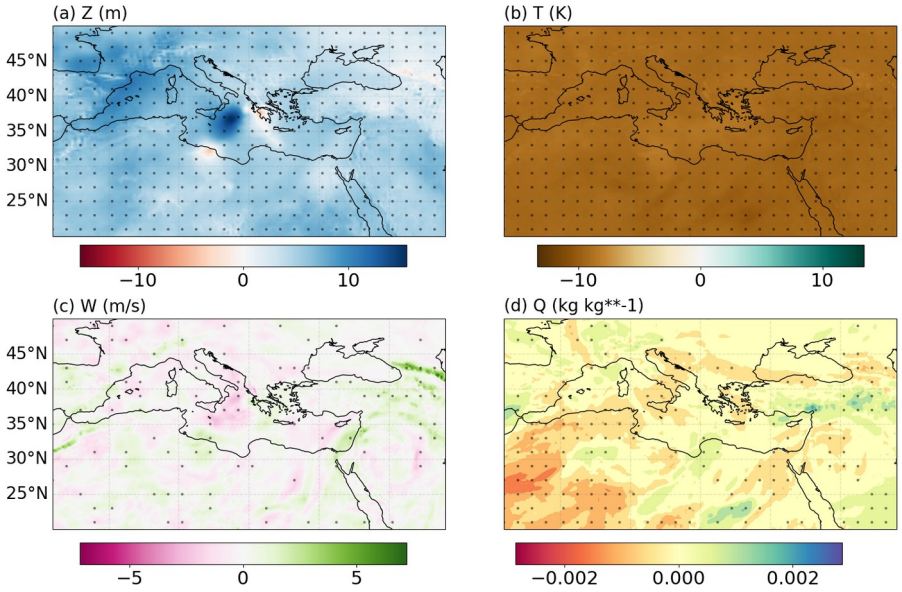

Figure S3: Mean Bias Error (MBE) of the WRF model configuration with grid nudging applied above the planetary boundary layer (PBL), evaluated against ERA5 reanalysis data at 1000 hPa for various atmospheric variables. Statistically significant differences, determined at the 95% confidence level using the Wilcoxon signed-rank test, are marked with dots.

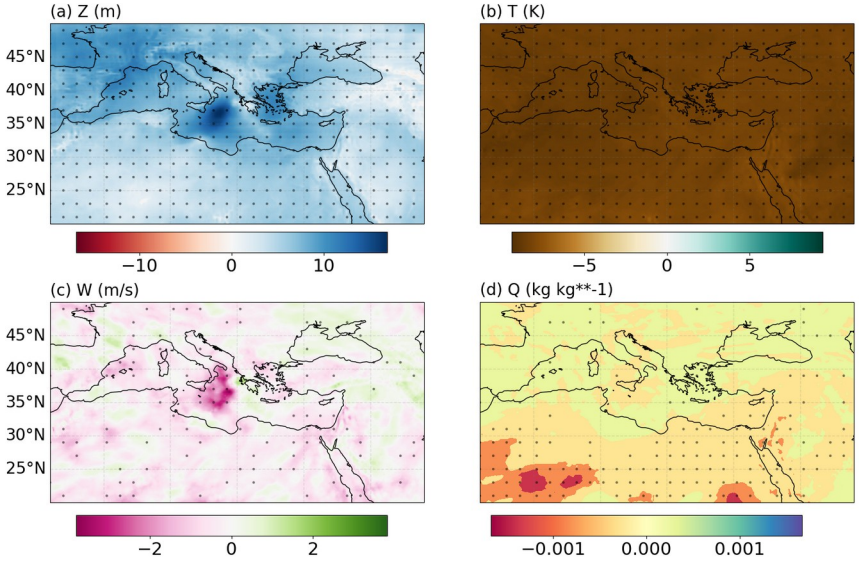

Figure S4: Similar to Figure S3, but for 850 hPa.

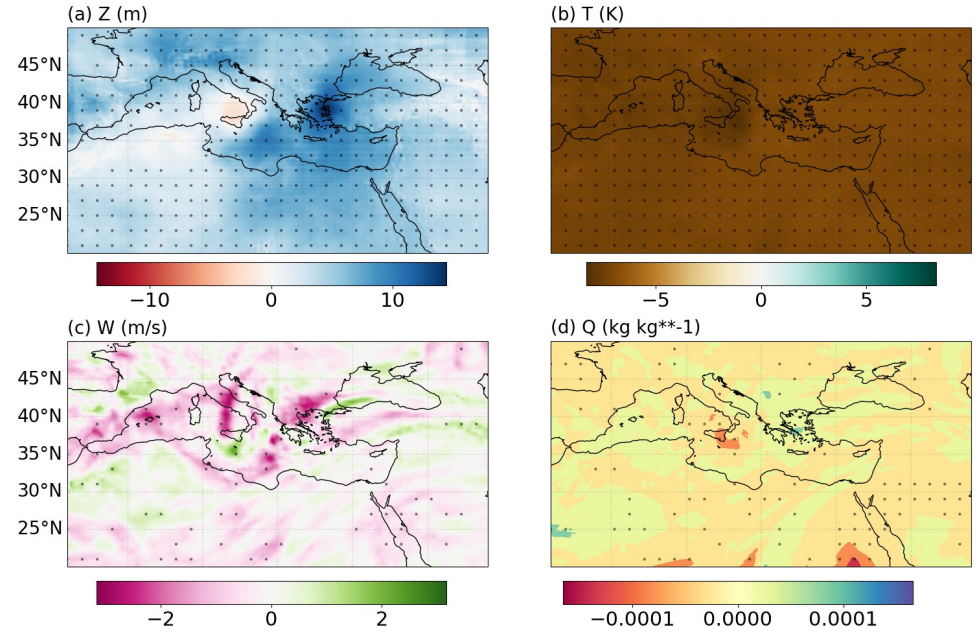

Figure S5: Similar to Figure S3, but for 500 hPa.

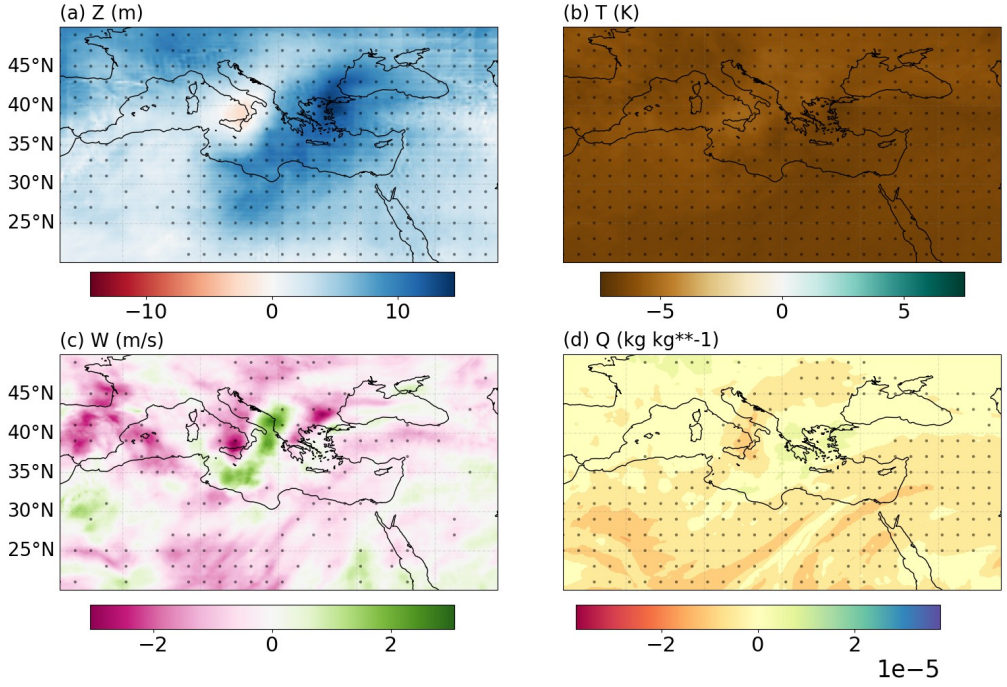

Figure S6: Similar to Figure S3, but for 200 hPa.

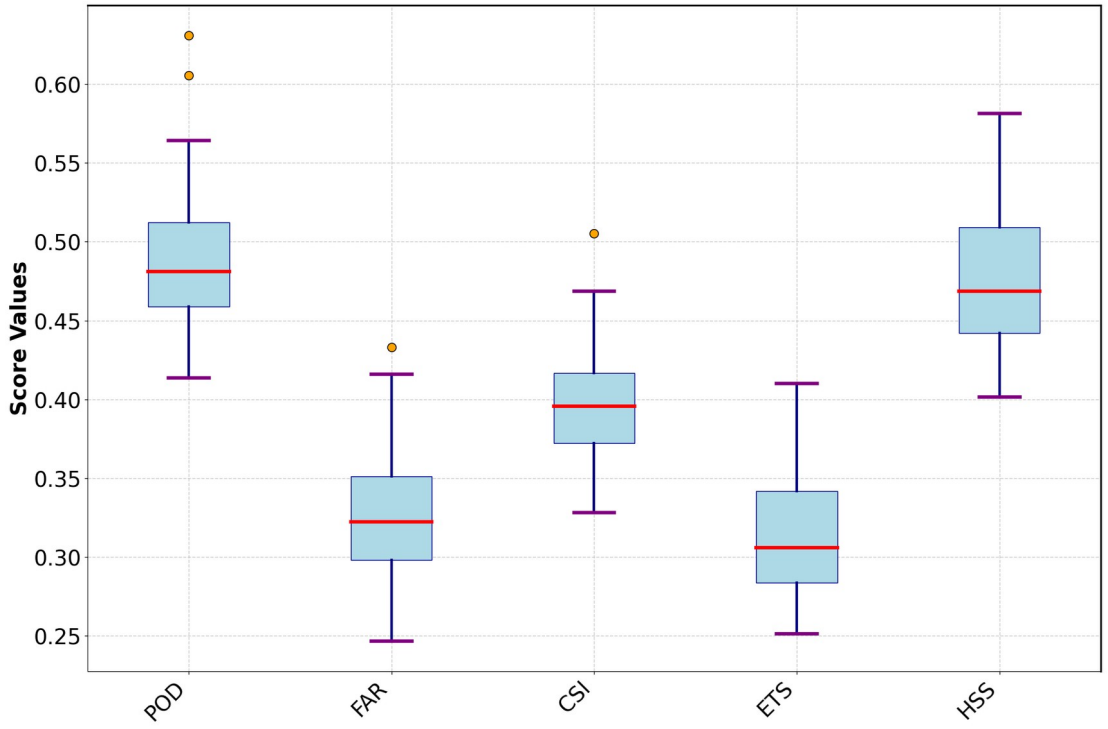

Figure S7: Spatial verification of precipitation for the WRF model configuration with gridded nudging above the PBL. The reference dataset used is the Multi-Source Weighted-Ensemble Precipitation (MSWEP, Beck et al., 2019). The figure presents several performance metrics: Probability of Detection (POD), where a value of 1 indicates perfect detection; False Alarm Ratio (FAR), where a value of 0 indicates no false alarms; Critical Success Index (CSI), with a value of 1 representing a perfect forecast; Equitable Threat Score (ETS), where values approaching 1 indicate perfect prediction (no false alarms, no misses), and values near 0 suggest random chance; Heidke Skill Score (HSS), where a score of 1 indicates perfect skill and a value of 0 reflects performance no better than random chance, with negative values indicating worse than random performance.

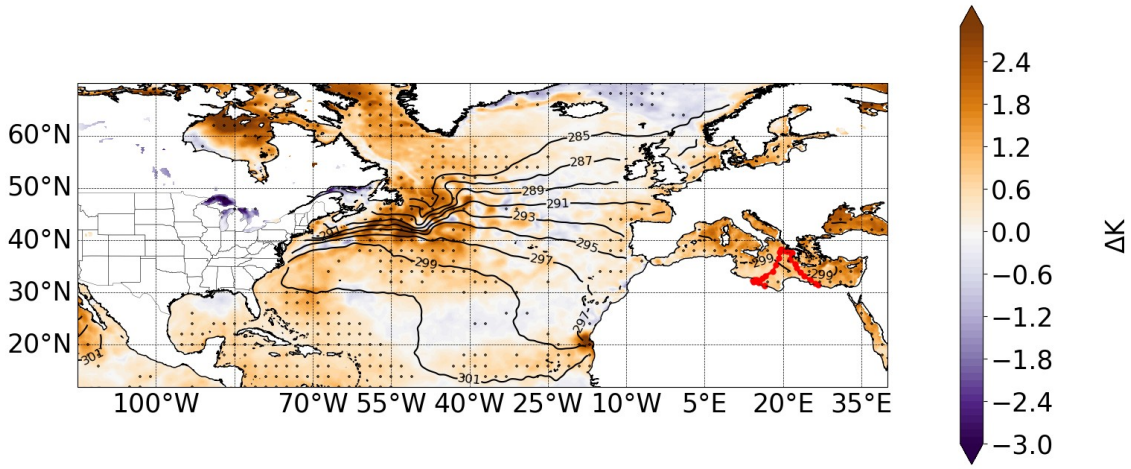

Figure S8: Climatological Sea Surface Temperature (SST) anomalies from ERA5 (shaded) during the lifespan of Storm Ianos (14–20 September 2020) over the North Atlantic Ocean and the Mediterranean Sea. The storm track is shown in red. Contours represent the mean ERA5 SST during Ianos' lifetime, and markers indicate significant anomalies exceeding 2 standard deviations.

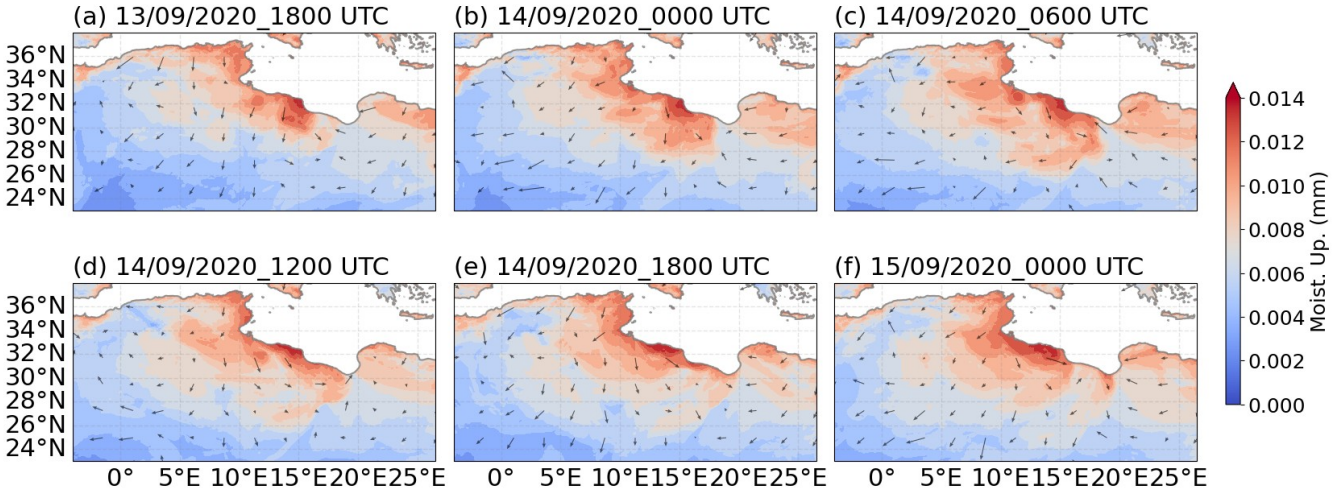

Figure S9: Mean Water Vapor Mixing Ratio (QVAPOR) averaged between 1000 and 750 hPa, with surface winds represented by arrows, during the early stages of Ianos' lifecycle.

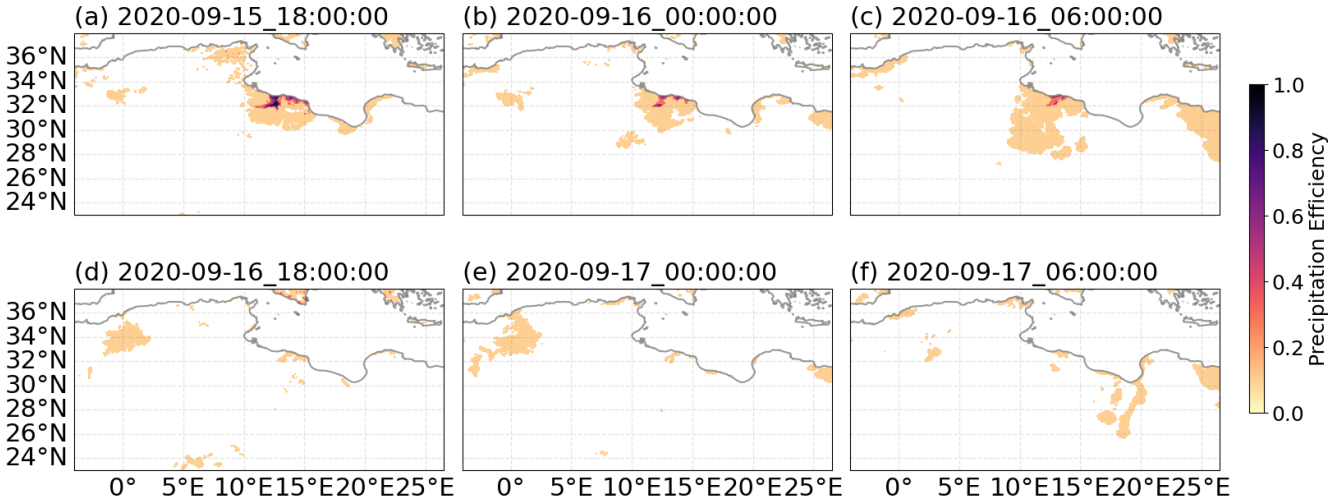

Figure S10: Precipitation efficiency over land in northern Africa.

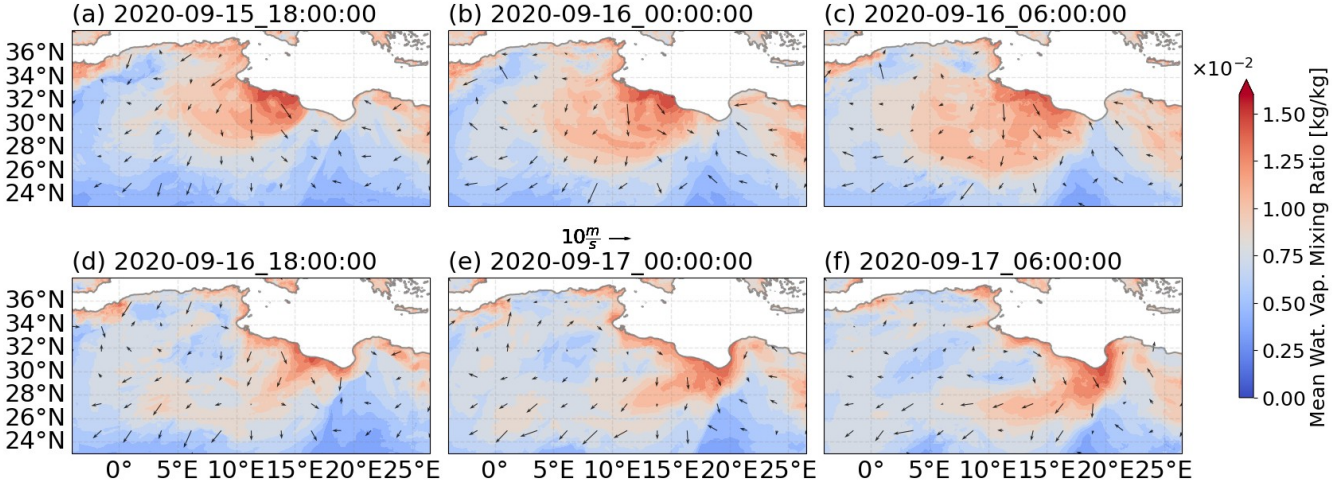

Figure S11: Mean Water Vapor Mixing Ratio (QVAPOR) averaged between 1000 and 750 hPa, with surface winds represented by arrows, during the intensification and mature stages of Ianos.

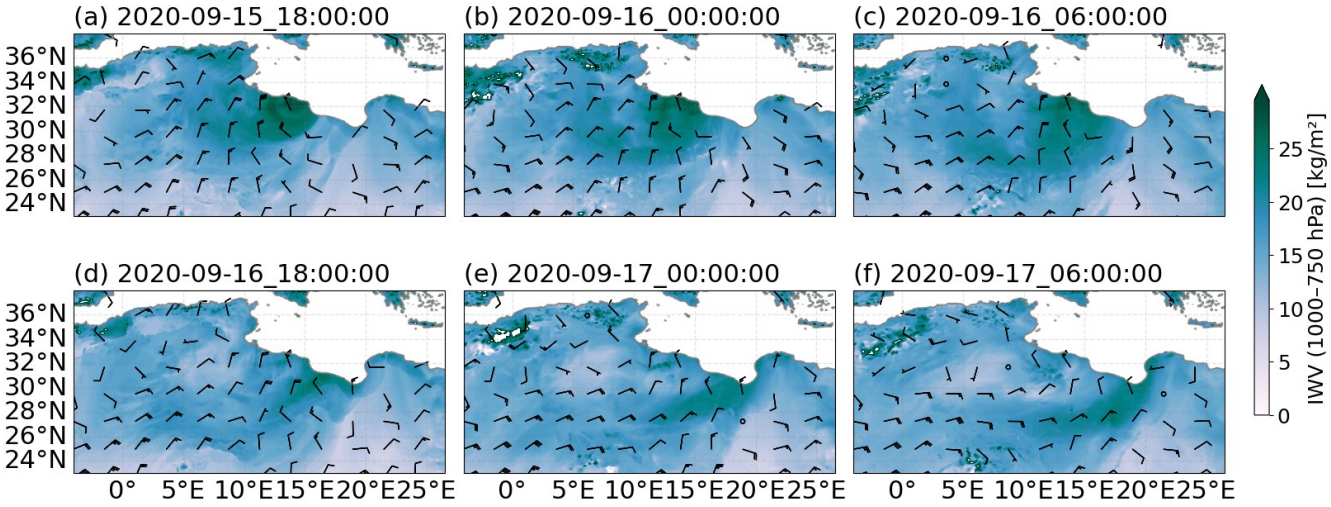

Figure S12: Integrated Water Vapor Column (kg/m²) between 1000 and 750 hPa, with surface winds represented by arrows, during the intensification and mature stages of Ianos.

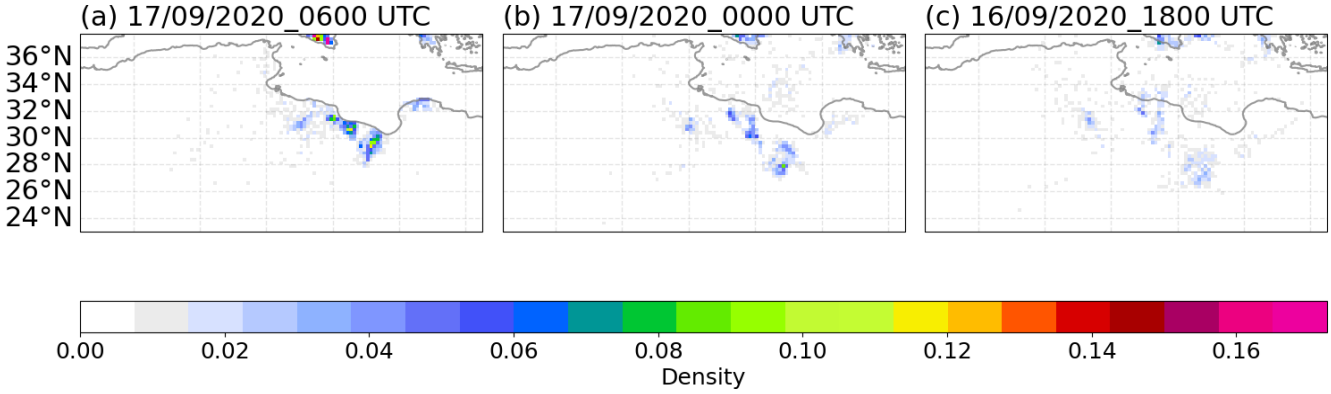

Figure S13: Precipitating particle density over northern Africa, along their backward trajectory starting on September 17, 0600 UTC.

Reference

Beck, H. E., E. F. Wood, M. Pan, C. K. Fisher, D. G. Miralles, A. I. J. M. van Dijk, T. R. McVicar, and R. F. Adler, 2019: MSWEP V2 Global 3-Hourly 0.1° Precipitation: Methodology and Quantitative Assessment. Bull. Amer. Meteor. Soc., 100, 473–500, https://doi.org/10.1175/BAMS-D-17-0138.1.